Effects of Tides and Storm Surges on North Sea Wind Waves

HENDRIK L. TOLMAN

Department of Civil Engineering, Delft University of Technology, Delft, The Netherlands

(Manuscript received 6 July 1990, in final form 28 November 1990)

ABSTRACT

Effects of tides and storm surges on wind waves in shelf seas are assessed by hindcasting three North Sea storm cases. It is shown that tides and storm surges in shelf seas should be considered as an unsteady medium for wind wave propagation if wave–current interactions are assessed. Tides mainly result in oscillations of mean wave parameters, whereas surges result in systematic variations. Due to accumulation of effects, small wind-induced currents might have a larger impact on wave parameters than larger but oscillating tidal currents. Although these results are obtained from typical North Sea conditions, it is expected that they are fairly representative for tides and surges in shelf seas in general. For the North Sea relatively small tide and surge-induced modulations of mean wave parameters such as the significant wave height or the mean wave period have been found (typically 5% to 10%). Modulations of the spectral density of the wave energy can be of the order of 50% to 100%. Effects of current refraction appear to be negligible, whereas effects of bathymetry-induced refraction is locally distinct in extreme wind and wave conditions. Observed modulations of mean wave parameters in the storm cases considered here appear to be mainly wind induced.

1. Introduction

Wave–current interactions, in particular the influences of currents on waves, have been the subject of several theoretical investigations in the last decades. After some pioneering papers by Unna (1941, 1942, 1947) and Barber (1949), the theory for wave–current interaction was developed by Longuet-Higgins and Stewart (1960, 1961, 1962), who introduced the concept of radiation stress, and by Whitham (1965) and Bretherthon and Garrett (1968), who introduced the concept of action conservation. The theory is now well established and treated in numerous textbooks, review papers and reports (e.g., Whitham 1974; Peregrine 1976; Phillips 1977; Mei 1983; Peregrine and Jonsson 1983; Jonsson 1990). Wave–current interactions are for a major part governed by depth- and current-induced changes of wavenumber and wave frequency. Such changes depend on the character of the variations of depth and current: variations in space result in changes of the wavenumber, whereas variations in time result in changes of the absolute frequency, i.e., the frequency as observed from fixed locations (e.g., Mei 1983, p. 96). The literature on wave–current interactions is mostly concerned with small scale areas, for which the (tidal) depth and current field are assumed to be quasi-stationary with respect to the travel time of wind waves, or with large-scale areas with quasi-stationary ocean current systems such as the Gulf Stream. In these cases a quasi-stationary approach is feasible, in which the absolute frequency is assumed to remain constant during propagation. To the knowledge of the author, only a few applications for unsteady depths and currents have been presented. Wave–current interactions in such cases are (properly) treated by Unna (1941), Barber (1949) and Longuet-Higgins and Stewart (1960). In several recent papers, however, effects of unsteadiness are not accounted for, but a quasi-stationary approach is used even for currents that are explicitly stated to be unsteady ("nonstationary") currents (e.g., Chen and Wang, 1983).

Considering the above, the subject of wave–current interactions for large scale, unsteady depths and currents seems to be poorly investigated.[1] Tides and surges in shelf seas as considered in this study represent such unsteady depth and current conditions, because the typical travel time of wind waves through shelf seas (order of magnitude of a few days) is much larger than the time scale of current and depth variations (typically 12 h).

For highly academic situations the importance of unsteadiness of tidal currents for wave–current interactions is shown by Tolman (1990b). This study aims to assess the relative importance of the unsteadiness of tides for practical shelf sea conditions and to compare effects of tides and surges. By hindcasting three North

Corresponding author address: Dr. H. L. Tolman, Code 911, NASA/Goddard Space Flight Center, Greenbelt, MD 20771.

[1] Parallel to this study, Yamaguchi et al. (1989) and Yamaguchi and Hatada (1990) studied wind wave propagation over unsteady currents, neglecting source terms.

Sea storm cases, results are obtained that are expected to be fairly representative for shelf seas in general. From these hindcasts the magnitude of effects of interactions is also estimated and finally a comparison with measurements is presented to estimate to which extent tides are responsible for observed modulations of mean wave parameters (another source for observed modulations is obviously the wind).

Wave height modulations measured in the southern North Sea as presented by Tolman (1988, 1990b) suggest that effects of currents on waves can be significant, whereas studies of wave-driven currents suggest that the significant effects of waves on currents mainly occur in the surf zone. Therefore, only effects of tides and surges on wind waves (and not vice versa) will be considered here.

The hindcasts have been performed with the model WAVEWATCH (Tolman 1989, 1990a, 1991), which was specially developed for this study. This model is briefly described in section 2. Currents, water levels and wave boundary conditions for this model are calculated with previously available numerical models (section 2). Selected hindcast results are presented in section 3, and the results are discussed in section 4.

2. Numerical models

Wind wave hindcasts for this study have been performed with the numerical wave model WAVEWATCH, which has been developed specially for this study. This model contains all large-scale effects of wave–current interactions as well as (explicit) source terms for wave growth, decay and nonlinear wave–wave interactions. A detailed description is given by Tolman (1989, 1990a, 1991). The physics of the model will be discussed here only as far as they are relevant for the discussion of the present results. For numerics of the model reference is made to the above three papers.

Random wind waves are generally described with a spectrum giving energy or variance density as a function of wavenumber k, frequency f and direction θ (normal to the crest of the spectral component). In the linear theory of surface gravity waves, wavenumber and frequency are interrelated in the dispersion relation.

$$\omega = \sigma + \mathbf{k}\cdot\mathbf{U}, \tag{1}$$

$$\sigma^2 = gk\tanh kd, \tag{2}$$

where ω ($=2\pi f_a$) is the absolute radian frequency, as observed in a frame of reference fixed to the bottom and σ ($=2\pi f_r$) is the relative frequency, as observed in a frame of reference that moves with the mean current velocity $\mathbf{U}$. The water depth is denoted as d (local average over the wave field), $\mathbf{k}$ is the wavenumber vector with absolute value k and direction θ, and g is the acceleration of gravity. In WAVEWATCH the wind waves are described using the variance density spectrum $F(\omega, \theta)$. Changes of this variance density due to propagation over varying depths and currents are described using the following action balance equation:

$$\frac{\partial N}{\partial t} + \nabla_x\cdot[(\mathbf{c}_g + \mathbf{U})N] + \frac{\partial}{\partial\theta}[c_\theta N] + \frac{\partial}{\partial\omega}[c_\omega N] = \frac{S}{\sigma}, \tag{3}$$

$$c_g = \frac{\partial\sigma}{\partial k} = n\frac{\sigma}{k}, \quad n = \frac{1}{2} + \frac{kd}{\sinh 2kd}, \tag{4}$$

$$c_\theta = -\frac{1}{k}\left[\frac{\partial\sigma}{\partial d}\frac{\partial d}{\partial m} + \mathbf{k}\cdot\frac{\partial\mathbf{U}}{\partial m}\right], \tag{5}$$

$$c_\omega = \frac{\partial\sigma}{\partial d}\frac{\partial d}{\partial t} + \mathbf{k}\cdot\frac{\partial\mathbf{U}}{\partial t}, \tag{6}$$

where $N = F/\sigma$ is the action density spectrum and S represents the net effect of sources and sinks for wave variance (e.g., wind input). The left-hand side of Eq. (3) represents the local rate of change of the action density (first term) and effects of propagation. The second term on the left-hand side represents rectilinear propagation in the geographic space (including energy exchanges between wind waves and the mean current), the third term represents refraction and the fourth term represents frequency shifts due to the unsteadiness of depth and current (e.g., Mei 1983, p. 96). The right-hand side of Eq. (3) represents all effects of wave generation and dissipation, including wave generation by wind (Snyder et al. 1981), nonlinear resonant wave–wave interactions (Hasselmann 1960; Phillips 1960), whitecapping (Komen et al. 1984) and wave energy dissipation due to bottom friction (Madsen et al. 1988). The actual formulations are those of the WAM model (WAMDI Group 1988), except for the formulation of the bottom friction. To account for effects of currents on the source terms, the source terms have been formulated in a frame of reference moving with the mean current. This introduces minor adaptations to account for the wind speed in the moving frame and the effects of the currents on the wave bottom boundary layer (see Tolman 1990a, 1991).

To perform calculations with the numerical wave model, a bottom grid, wind fields, depth and current fields and wave boundary conditions at upwind model boundaries are required. The North Sea bathymetry as used in this study is presented in Fig. 1. Model wind fields consist of UK6 wind fields of the British Meteorological Office (BMO). Depth and current fields have been calculated with the numerical model DUCHESS (e.g., Wang 1989, depth integrated shallow water equations), using both wind forcing and typically six tidal constituents at the open boundaries (taken from Voogt 1985). Hence the depth and current fields describe both tides and surges. For northwesterly storms, wave boundary conditions for the northern boundary have been calculated with the deep-water no-current ocean wave model DOLPHIN (Holthuijsen and De

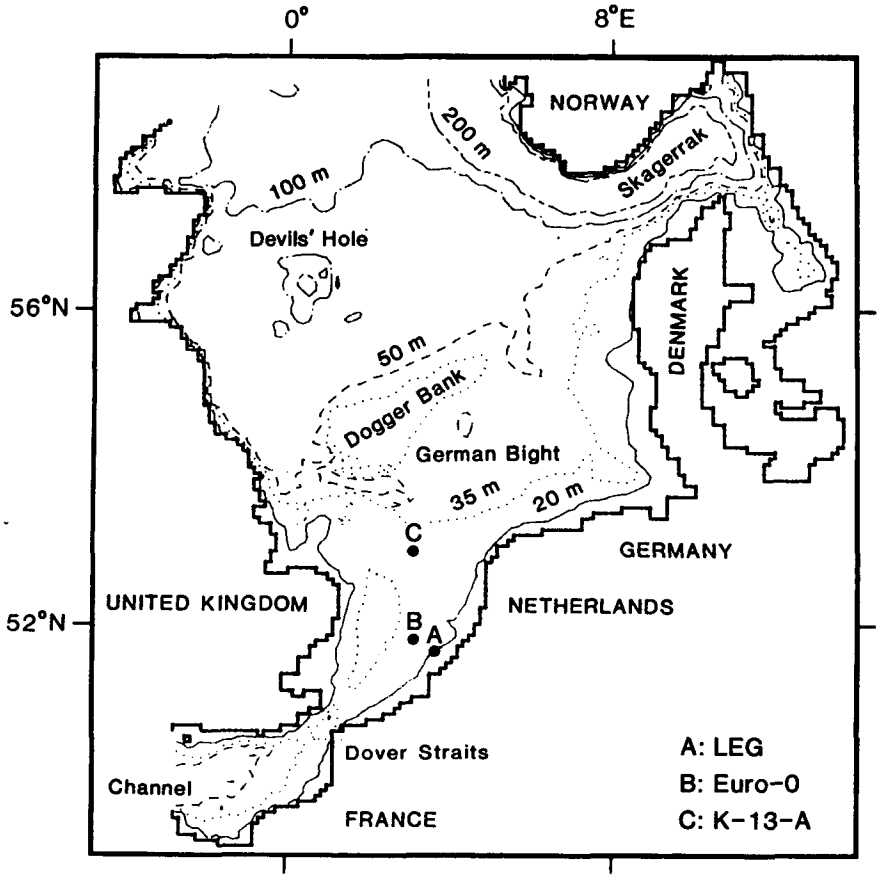

FIG. 1. The North Sea bottom contours and locations.

Boer 1988). The layout of the grids for the different models is shown in Fig. 2, and information on discretizations is gathered in Table 1.

3. North Sea case studies

a. Introduction

As mentioned in the Introduction, the main attention of this study is focused on the specific effects of the unsteadiness of tidal depths and currents on wind waves. This subject is studied by hindcasting the North Sea storm cases as discussed in section 3b. Similarly the differences between effects of tides and surges and the magnitude and spatial distribution of effects of tides and surges on wind waves are analyzed. Finally hindcasted modulations of wave parameters are compared with observed modulations, to estimate to what extent tides are responsible for observed modulations. The main attention is focused on the southern North Sea since the largest current velocities (and therefore probably the largest effects of interactions) occur in this region. The nature of the current fields for the North Sea is illustrated here with current fields and maximum current velocities for an arbitrary day of one of the cases considered here (Figs. 3 and 4 respectively).

To perform the above numerical investigations, several model versions of WAVEWATCH have been used, in which different effects of tides and surges on waves are either incorporated or neglected. For all cases considered here, hindcasts have been performed with all model versions as discussed below. In the reference version of the model (denoted as version A), all effects of tides and surges are taken into account. The total effects of wave–current interactions are assessed by comparing the results of this reference version with the results of a model version in which tides and surges are neglected (denoted as version C). Similarly, the effect of a single mechanism (e.g., refraction) is estimated by comparing results of the reference version A with results of a model version in which the corresponding mechanism is neglected. In such a way effects of unsteadiness, refraction, currents and surface level variations are investigated (versions B_1 through B_4, see Table 2).

Measured wind and wave data in the southern North Sea were available for the locations LEG, Euro-0 and K-13-A (see Fig. 1 and Table 3). The wind data at LEG are used in combination with the wave data at Euro-0. The wind data consist of wind speeds and directions at 10 m altitude. The wave data consist of

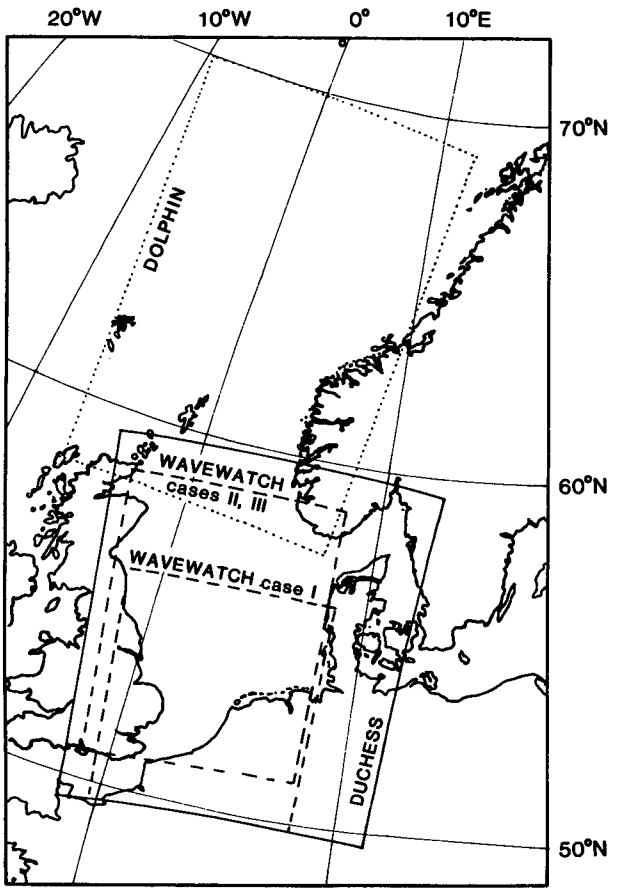

FIG. 2. Layout of grids for WAVEWATCH, DUCHESS and DOLPHIN (DOLPHIN is used for the NW winds of cases II and III only).

measurements with WAVEC buoys (e.g., Van der Vlugt 1984). To limit the number of data presented here, interactions are analyzed in detail for the locations Euro-0 and K-13-A only.

The analysis considers integral parameters of the wave spectrum, i.e. the significant wave height H_s, the mean absolute period T_a, the mean relative period T_r and the mean direction $\bar{\theta}$:

$$H_s = 4\left(\iint F(\omega, \theta)d\omega d\theta\right)^{1/2}, \tag{7}$$

$$T_a = \overline{2\pi/\omega}, \tag{8}$$

$$T_r = \overline{2\pi/\sigma}, \tag{9}$$

$$\bar{\theta} = \arctan \frac{\iint \sin\theta F(\omega, \theta)d\omega d\theta}{\iint \cos\theta F(\omega, \theta)d\omega d\theta}, \tag{10}$$

where the overbar denotes the average over the variance density spectrum $F(\omega, \theta)$, which for some arbitrary parameter z is given as

$$\bar{z} = \frac{\iint z(\omega, \theta)F(\omega, \theta)d\omega d\theta}{\iint F(\omega, \theta)d\omega d\theta}. \tag{11}$$

Modulations of the isolated energy in fixed frequency bands will be discussed briefly.

b. *Case description*

Three storm cases of the storm season 1987–88 are considered. Cases I and II show tide-dominated conditions and case III shows a significant surge.

Case I consists of a series of moderate southwesterly storms (Beaufort 7) in the southern North Sea in the period 1–4 January 1988. These storms are caused by four consecutive depressions moving over the northern North Sea. Case II consists of one moderate northwesterly storm (Beaufort 6 to 7) in the entire North Sea in the period 26–28 September 1987. This storm is caused by a stationary high pressure area over Ireland and a stationary depression over the northern Baltic Sea. These two cases have been selected to assess wave–tide interactions for different wind (wave) directions and to compare model results with measurements.

Case III consists of an extreme northwesterly storm (Beaufort 10 to 12) over the entire North Sea during the period 28 and 29 February 1988, caused by a high pressure area over the Atlantic and a low pressure area over Norway. No continuous wave data were available for this case.

The tidal range in the southern North Sea is typically 1.5 m, and the tidal currents are typically 0.5 to 1.0 m

TABLE 1. Grid increments.

	Space	Time	Spectra
Wind waves (WAVEWATCH)	24 km × 24 km	15 min	24 directions, $\Delta\theta = 15°$ 26 frequencies, 0.041 Hz – 0.453 Hz $f_a^{n+1} = 1.1 f_a^n$
Depth and current (DUCHESS)	8 km × 8 km	7.5 min	Not relevant
Wave boundary conditions (DOLPHIN)	1° × 1° (appr.)	1.5 h	As in WAVEWATCH
Wind fields (UK6)	1° × 1°	3 h (output)	Not relevant

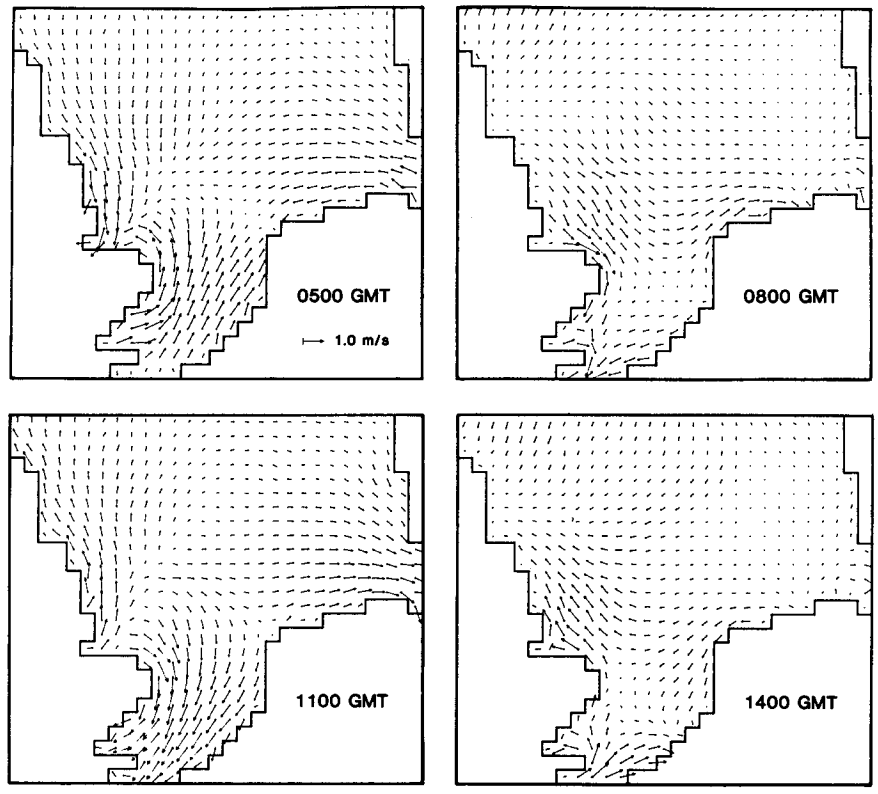

FIG. 3. Current fields for several times on 26 September 1987.

s^{-1} (see e.g., Fig. 4). Cases I and II are near spring tide, and case III is near neap tide. In cases I and II the storm surge is negligible (i.e., less than 0.2 m in elevation and less than 0.05 m s^{-1} in current). In case III the storm surge is significant, as is illustrated in Fig. 5.

In cases II and III significant wave energy enters the northern North Sea from the Norwegian Sea. This makes the explicit calculation of wave conditions at the northern model boundary necessary.

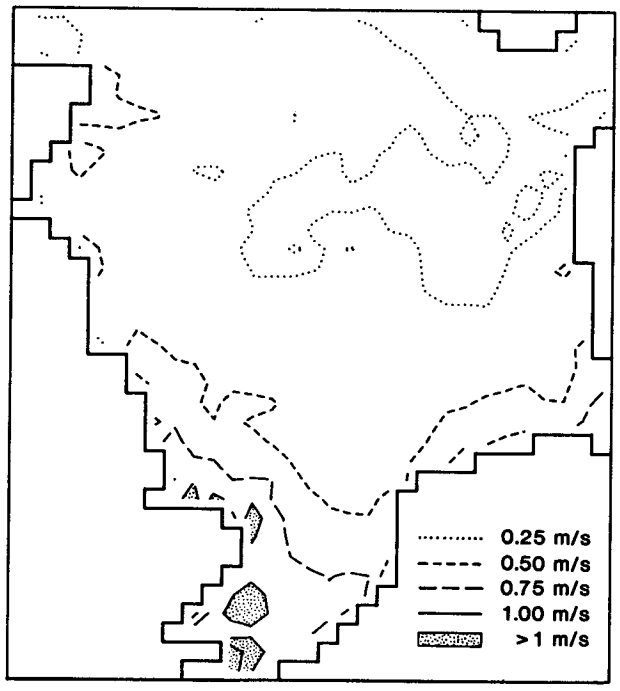

FIG. 4. Maximum current velocities on 26 September 1987.

c. *Numerical investigations*

1) EFFECTS OF TIDES ON WIND WAVES

Effects of tides are analyzed by considering the results of cases I and II in which no significant surges occur. In these moderate conditions waves are essentially in deep water so that surface level variations do not con-

TABLE 2. Definition of versions of WAVEWATCH.

Version	Description
A	Including all effects of tides and surges.
B_1	Without frequency shifts due to the unsteadiness of depth and current.
B_2	Without depth and current refraction.
B_3	Without (tide- and surge-induced) currents, i.e. surface level variations only.
B_4	Without (tide- and surge-induced) surface level variations.
C	Without tides and surges, but including bathymetry-induced shallow water effects (depth shoaling and depth refraction).

TABLE 3. Locations.

Location	Coordinates	Depth (m)	Wind data	Wave data
LEG	51°55'N, 3°40'E	20	Yes	No
Euro-0	52°00'N, 3°16'E	26	No	Yes
K-13-A	53°13'N, 3°13'E	29	Yes	Yes

tribute to interactions. The latter is confirmed by the numerical model since the model versions with all interactions and with currents only (versions A and B_4, see Table 2) result in practically identical values of mean wave parameters. Consequently interactions are essentially caused by (tidal) currents.

The tidal currents result in relatively small but recognizable modulations of the wave height H_s and the wave periods T_a and T_r, as is illustrated in Fig. 6 for locations Euro-0 and K-13-A in case I. In this figure tide-induced modulations are observed as the difference between the solid lines (with tides) and the dotted lines (without tides). The effects of the tidal currents show a clear modulation with the period of the tide, in particular at Euro-0. The mean wave direction $\bar{\theta}$ (not presented here) shows negligible effects of the tidal currents (tide-induced modulations of less than 1°). Consequently effects of refraction appear to be negligible for Euro-0 and K-13-A in cases I and II. This was expected for depth refraction since waves are essentially in deep water. For current refraction this is less obvious but not unreasonable since gradients in tidal currents are generally small in this area (see e.g., Fig. 3).

Since effects of tidal currents on mean wave parameters are relatively small, they are isolated to allow for a more detailed analysis. This is achieved by simply considering the differences in the results obtained with and without tides (and surges). For the significant wave height H_s, the modulation ΔH_s for a given time and place is calculated as

$$\Delta H_s = H_{s,A} - H_{s,C}, \tag{12}$$

where the suffixes A and C indicate results of model versions A and C. Modulations of the absolute and relative period (ΔT_a and ΔT_r, respectively), are defined similarly. Such modulations are particularly interesting in relation with the local current velocity, since such a relation can show to which extent tide-induced modulations can be estimated using local currents only. In such a comparison, the current velocity U_p in the mean propagation direction of the waves is more relevant than the overall current velocity U, as follows directly from Eq. (1). The former velocity is defined here as

$$U_p = |\mathbf{U}| \cos(\theta_U - \bar{\theta}), \tag{13}$$

where θ_U is the current direction. In Figs. 7 and 8 the modulations of wave heights and wave periods at Euro-0 and K-13-A are presented as a function of the current velocity U_p. These figures show a clear hysteretic relation between the tide-induced modulations of mean wave parameters and the (tidal) current. This relation however, varies with place and case, so that it appears to be difficult to estimate effects of tides from the local tidal current only.

Modulations in fixed frequency bands of the spectrum can be much larger than the modulations of mean wave parameters. In any frequency band, relative modulations of the order of 50% have been found, as illustrated in Fig. 9, with results for Euro-0 in case I. In determining mean wave parameters, such intraspectral modulations largely cancel out.

2) EFFECTS OF UNSTEADINESS OF TIDAL CURRENTS

From the kinematics of wave trains it follows that unsteadiness of currents manifests as modulations of the absolute frequency or period, whereas inhomogeneity manifests as modulations of the relative frequency or period (e.g., Tolman 1990b). In the cases considered here, the unsteady nature of tidal currents results in modulations of the absolute periods, which are not negligible compared to modulations of the relative period. In fact, modulations of the absolute period dominate for most cases and locations, as illustrated in Figs. 6 and 8.

The relative importance of unsteadiness and inhomogeneity is most elegantly studied by analyzing how the local Doppler shift of Eq. (1) is balanced by modulations of either the absolute or the relative frequency, or alternatively, how the local current is related to modulations of either the absolute or the relative periods. For narrow-banded spectra the differences in (the

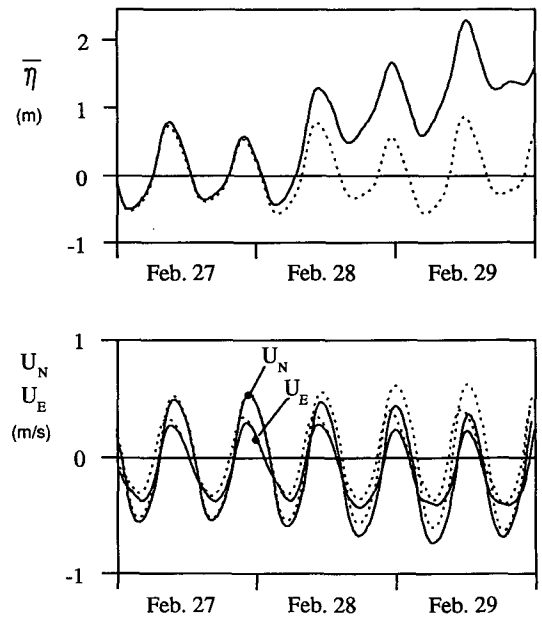

FIG. 5. Water levels $\bar{\eta}$ and current components U (suffixes N and E for northerly and easterly directions) for case III at location Euro-0. Solid line: with wind forcing; dotted line: without wind forcing.

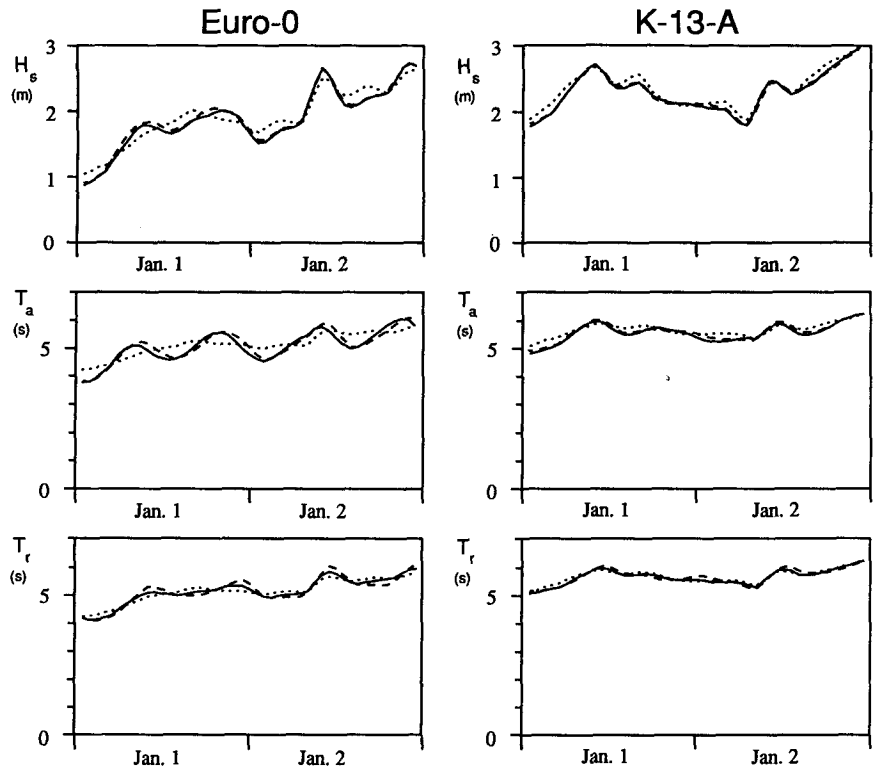

FIG 6. Mean wave parameters at locations Euro-0 and K-13-A for case I (1988). Solid line: with tides and surges; dotted line: without tides and surges; dashed line: with tides and surges, $d\omega/dt \equiv 0$ (quasi-stationary approach).

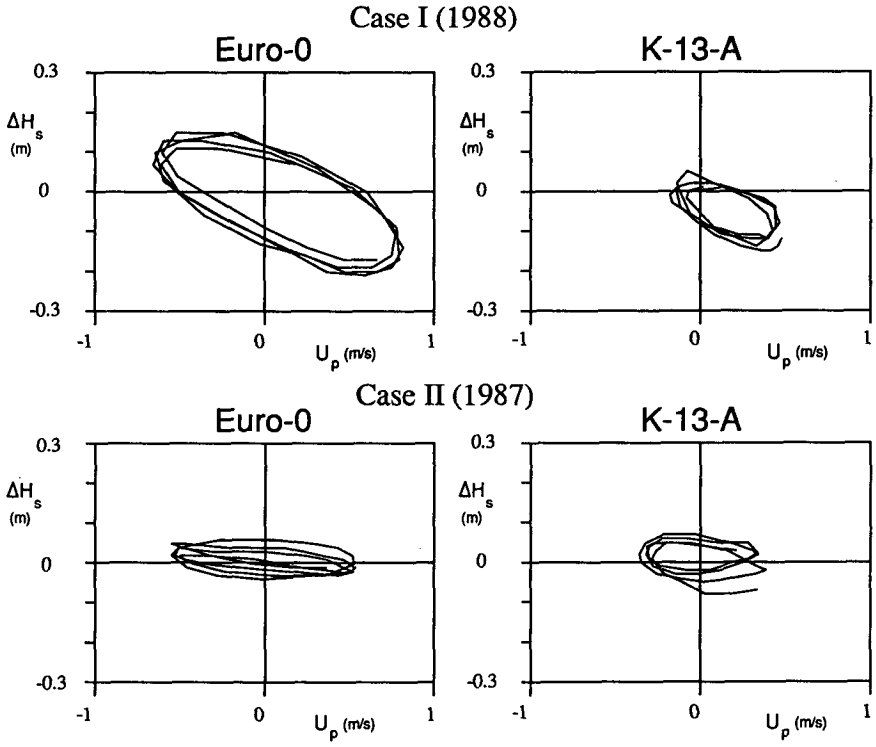

FIG. 7. Tide-induced modulations of the significant wave height ΔH_s as a function of the current velocity in the mean propagation direction of the waves U_p at locations Euro-0 and K-13-A for cases I and II.

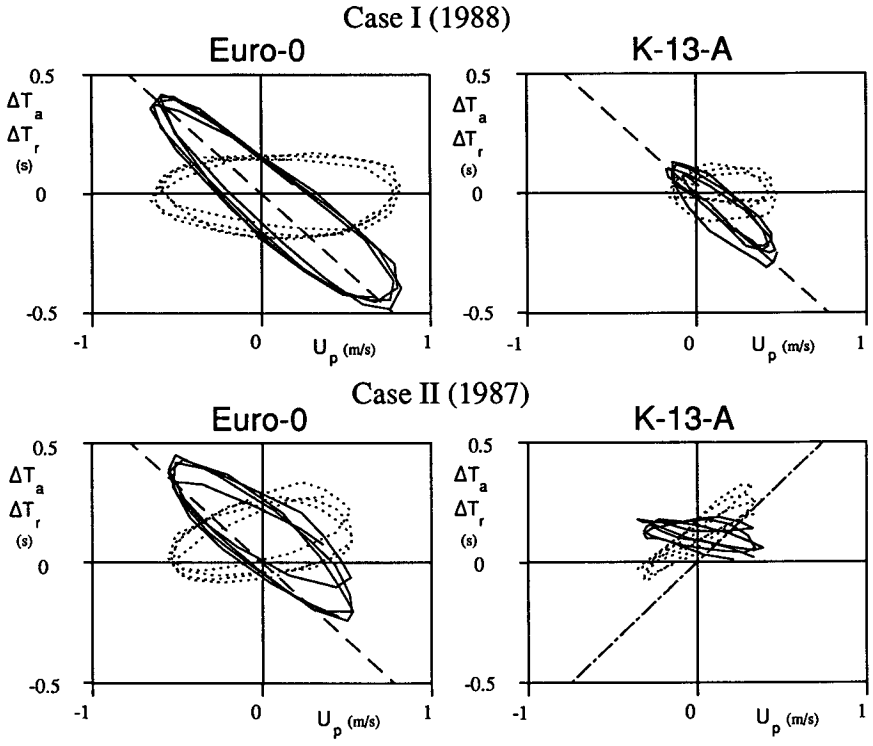

FIG. 8. Tide-induced modulations of the mean absolute period ΔT_a (solid lines) and the mean relative period ΔT_r (dotted lines) as a function of U_p at locations Euro-0 and K-13-A for cases I and II. Dashed line: Eq. (16) with $\Delta T_r \equiv 0$ (quasi-homogeneous approximation); dot-dash line: Eq. (16) with $\Delta T_a \equiv 0$ (quasi-stationary approximation). $\bar{k}d$ in Eq. (16) is estimated as the average for the location and hindcast considered.

modulations of) the absolute and relative periods are a function of the local current U_p, as will be shown below. For narrow-banded spectra, using Eq. (2), Eq. (1) becomes

$$\bar{\omega} = \bar{\sigma} + \bar{\sigma}^2[g \tanh\bar{k}d]^{-1}U_p, \qquad (14)$$

which, using Eqs. (8) and (9), can be written as

$$T_a = T_r\left(1 + \frac{2\pi}{g \tanh(\bar{k}d)T_r} U_p\right)^{-1}. \qquad (15)$$

For relatively weak currents, the second term within parentheses is much smaller than 1, in which case the difference between the modulations of the absolute and relative period becomes

$$\Delta T_a - \Delta T_r = T_a - T_r = \frac{-2\pi}{g \tanh\bar{k}d} U_p. \qquad (16)$$

Thus the difference between the (modulation of the) absolute and relative period follows directly from the local current U_p and the mean relative depth $\bar{k}d$.

A quasi-homogeneous approximation to this equation (i.e., $\Delta T_r \equiv 0$) can be used to estimate the modulation of the absolute period in cases where the effects of unsteadiness of the current dominate. At Euro-0 in cases I and II and at K-13-A in case I, such an equation indeed describes the trend of the modulation of the absolute period (see dashed line in Fig. 8). At K-13-A in case II, however, the modulation of the relative period dominates, suggesting a dominance of the inhomogeneity. The trend of the modulation of the relative period for this location and case is well described by a quasi-stationary approximation to Eq. (16), where $\Delta T_a \equiv 0$ (dash-dot line in Fig. 8). This inhomogeneous behavior appears to be related to the two-dimensional structure of the tide; waves approaching K-13-A from northwesterly directions travel through areas with large changes of current directions, resulting in large inhomogeneities of the current velocity U_p (see Fig. 3). For waves coming from southwesterly directions such inhomogeneities do not occur.

Two final remarks are made on the effects of unsteadiness of tidal depths and currents. First, modulations of the absolute period can also be caused in the generation and dissipation process due to tide-induced modulation of the relative wind speed or due to indirect effects of tide-induced modulations of relative frequencies and wavenumbers. This is illustrated in Fig. 6, where a modulation of the absolute period occurs, even if effects of unsteadiness are neglected in the calculations (i.e., in model version B_1, dashed lines). In

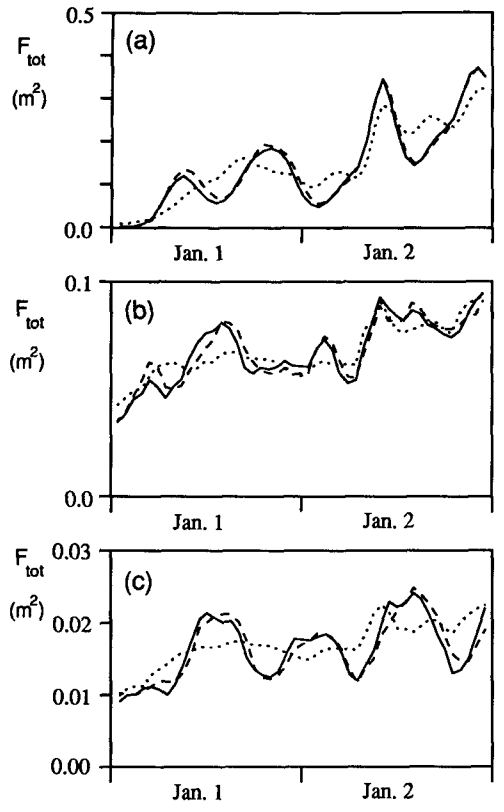

FIG. 9. Tide-induced modulation of wave energy in fixed absolute frequency bands (F_{tot}) at Euro-0 for case I. (a) 0.1–0.2 Hz (b) 0.2–0.3 Hz (c) 0.3–0.5 Hz. Legend as in figure 6.

case II, however, modulations of the absolute period disappear if the unsteadiness is neglected in the calculations (figures not presented here). Apparently unsteadiness is the only source for modulations of the absolute period in case II. Second, effects of unsteadiness on modulations of the wave height appear to be smaller than similar effects on the modulations of the wave periods, as is illustrated by the small differences between the dashed and solid lines for the wave height in Fig. 6.

3) SURGES VERSUS TIDES

Effects of surges are analyzed by considering the results of case III. In such severe wind and wave conditions, waves are essentially in shallow water, so that surface level variations can contribute to interactions (unlike in the moderate conditions of cases I and II). The numerical calculations indeed show effects of surface level variations and of currents on mean wave parameters, since results of calculations with and without tides and surges, with surface level variations only and with currents only (model versions A, C, B_3 and B_4, respectively) all show significant differences. This is illustrated in Fig. 10 with the wave heights and absolute periods at Euro-0 and K-13-A as calculated with the above model versions.

Since the time scale of computed interactions as presented in Fig. 10 (in particular those of the currents and water level variations separately, dash–double dot or dash–dot lines versus dotted lines) is clearly larger than that of the tide, the interactions appear to be surge dominated. For the effects of surface level variations this was expected since surface level variations are surge dominated (see Fig. 5). For the effects of currents this is somewhat surprising since local currents are still tide dominated (see Fig. 5). It seems that the systematic nature of small wind-driven currents results in more lasting (i.e., accumulated) effects than the larger, but oscillating tidal currents.

The higher surface level (Fig. 5) and corresponding larger depth due to the surge result in higher waves with longer periods (dash-dot lines versus dotted lines in Fig. 10). The increase in wave height and period is probably related to a reduced bottom-induced energy dissipation due to the increased water depth. On the other hand, currents reduce wave heights and periods (dash–double dot lines versus dotted lines in Fig. 10). This might be explained from the wind-induced currents, which in the southern North Sea are systematically in the propagation direction of the waves, reducing the effective fetch and wind speed. The separate contributions of surface level variations and currents to the interactions are opposite and largely cancel out, resulting in a practically negligible total effect of all interactions in this specific case.

4) SPATIAL DISTRIBUTION OF INTERACTION EFFECTS IN THE NORTH SEA

Results for Euro-0 and K-13-A as presented above show tide- and surge-induced modulations of wave heights and periods of typically 5% to 10%. Numerical calculations with a grid model make it possible to assess the spatial distribution of such effects. This is done here by considering the normalized rms differences between the local results of different model versions (i.e., the coefficient of variation CV). For example, the coefficient of variation of the wave height CV(H_s) is defined as:

$$\mathrm{CV}(H_s) = \frac{\left(T^{-1}\int [H_s - H_{s,\mathrm{A}}]^2\,dt\right)^{1/2}}{T^{-1}\int H_{s,\mathrm{A}}\,dt}, \quad (17)$$

where the suffix A denotes the results of the reference version (including all interactions) and where T is the duration of the averaging period (typically several tidal periods). The coefficient of variation is determined for the mean wave parameters H_s, T_a and T_r. For the mean direction $\bar{\theta}$ the normalization of the rms deviation is meaningless and it is therefore omitted. Since this study

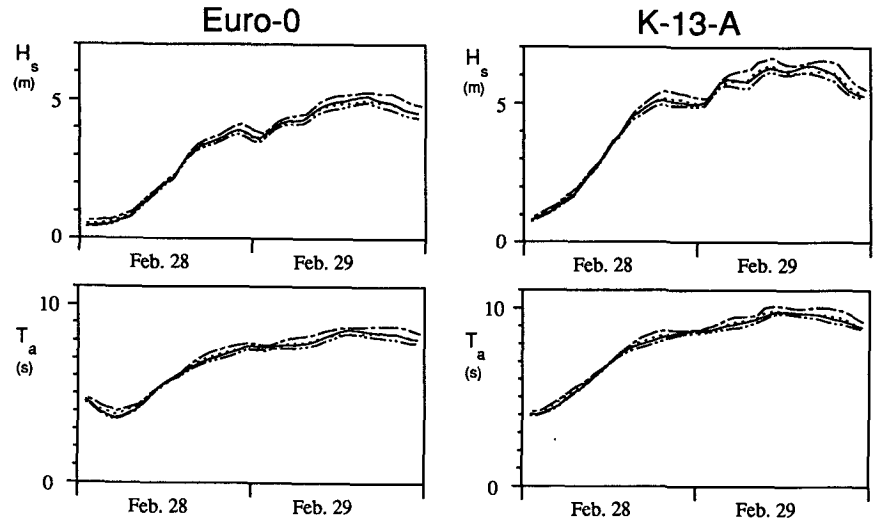

FIG. 10. Mean wave parameters at locations Euro-0 and K-13-A for case III (1988). Solid line: with tides and surges; dashed line: without tides and surges; dot-dash line: surface level variations only; dash-double dot line: currents only.

considers tides away from the coast only, shallow water coastal grid points are not considered in the presentation and the discussion of the results.

In general, areas with the largest effects of interactions roughly coincide with areas with the largest current velocities U_p in the mean propagation direction of the waves [Eq. (13)]. For case I, this is illustrated in Figs. 11 and 12, which show coefficients of variation for the wave height and absolute period (all interactions, model version A versus C) and extreme values of U_p, respectively. Coefficients of variations for the wave height are up to 15% near the Dover Straits and for the absolute period are up to 10%. For cases II and III coefficients of variation of, in particular, the wave

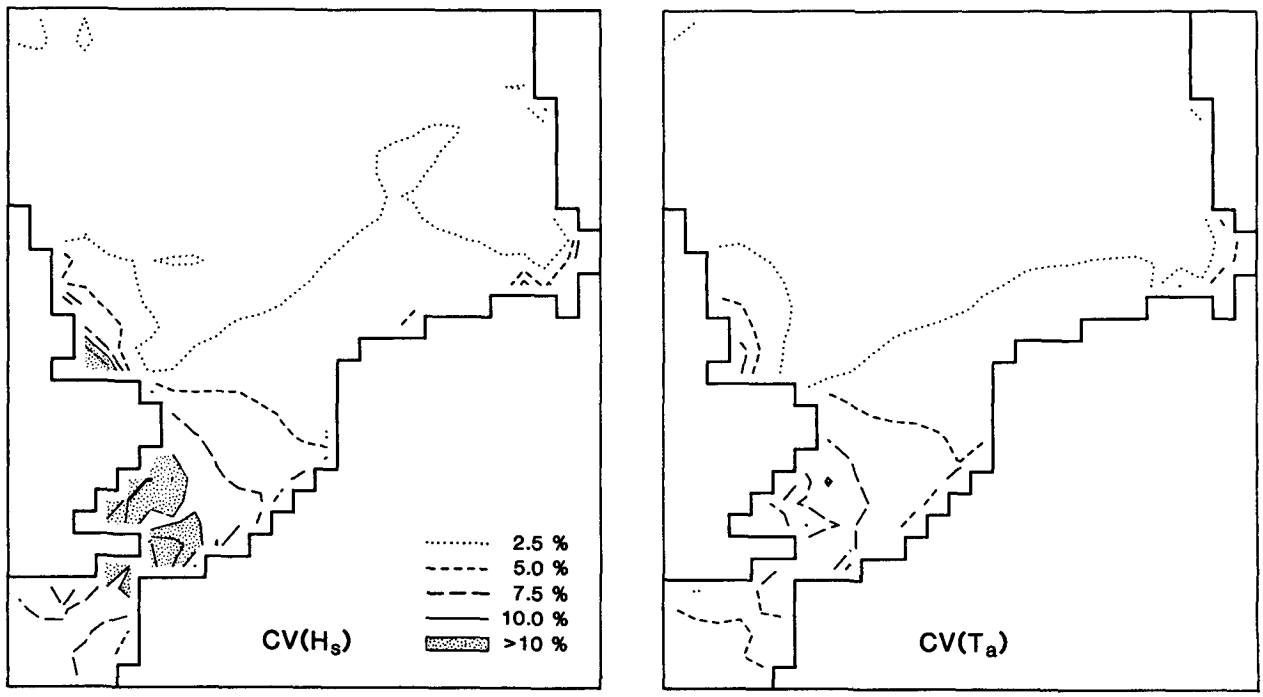

FIG. 11. Coefficients of variation of mean wave parameters for the total effects of wave–tide and wave–surge interactions (WAVEWATCH versions A and C), case I (1–2 January 1988).

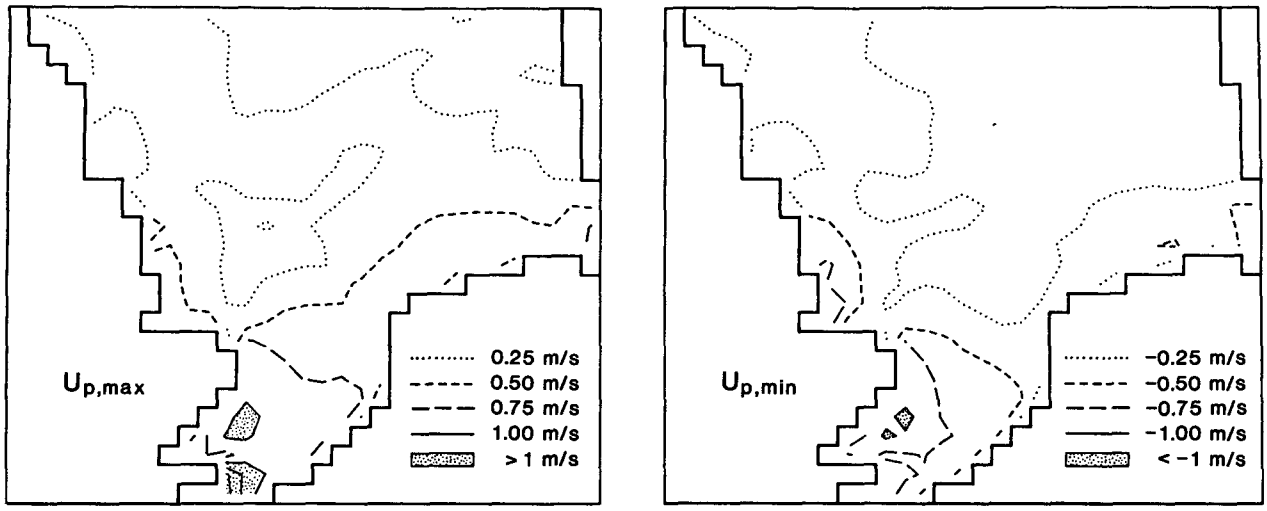

FIG. 12. Maximum and minimum current velocity in the propagation direction of the waves for case I (1–2 January 1988).

height are smaller, with largest values concentrated near the British east coast (figures not presented here).

Effects of unsteadiness show similar spatial distributions as the total effect of all interactions but, in general, are significantly smaller [(CV(H_s) < 4%, CV(T_a) < 7%, figures not presented here].

Effects of tides and surges on the mean direction are negligible for the entire North Sea in all three cases ($\Delta\bar{\theta}_{rms} < 2°$). Bottom-induced refraction is locally significant in extreme conditions ($\Delta\bar{\theta}_{rms}$ up to 15°), as is illustrated in Fig. 13 with the coefficient of variation of the wave height and the rms difference of mean wave direction for case III (model version A versus B_2; the reference version with all interactions and the model version without refraction, respectively). Since current refraction appears to be negligible and since surface level variations are obviously much smaller than bottom level variations, the thus-isolated differences are caused by bottom-induced refraction (representing a bias rather than a modulation). Locations with signif-

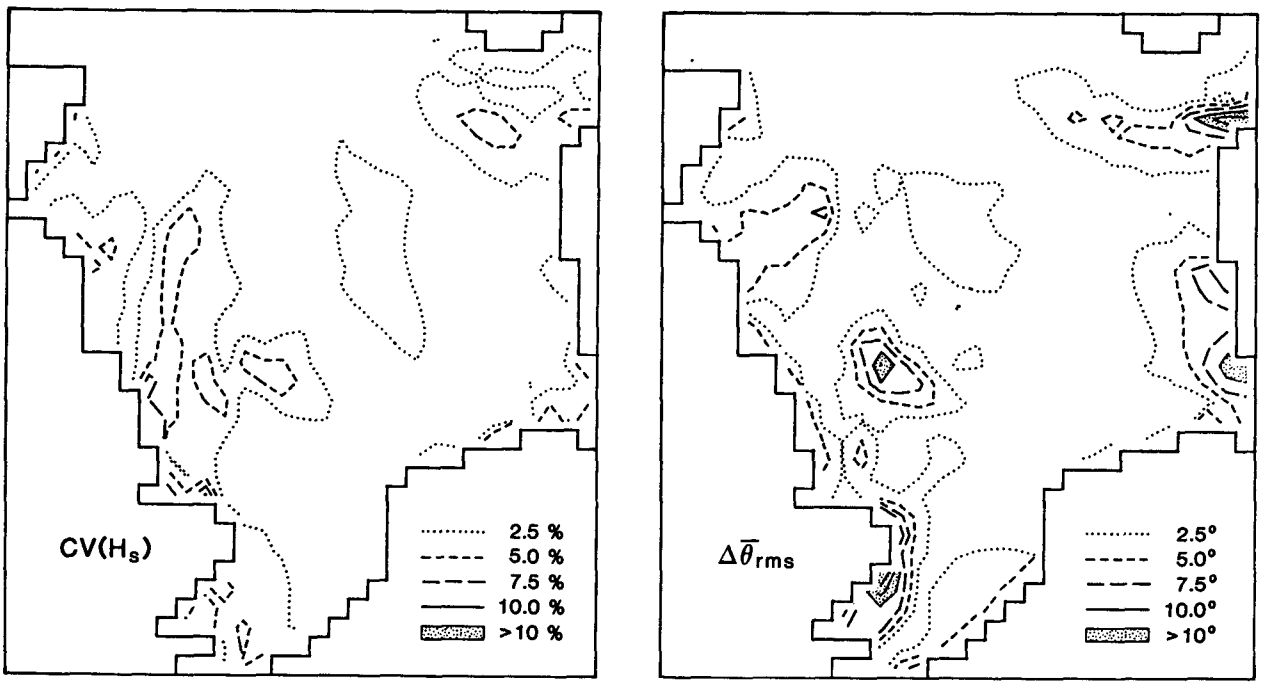

FIG. 13. Coefficient of variation of mean wave parameters and rms differences of the mean wave direction due to refraction for case III, 28–29 February 1988 (WAVEWATCH version A versus B_2).

icant effects are near areas with relatively shallow water and steep bottom gradients such as Dogger Bank, the Skagerrak and Devils Hole (see Fig. 1).

d. *Intercomparison of computed and observed modulations*

To estimate to which extent tides are responsible for observed modulations of mean wave parameters, calculated and observed modulations for the tide-dominated situations of cases I and II are intercompared. Calculated tide-induced modulations are obtained as in Eq. (12), and are marked with the suffix c (e.g., $\Delta H_{s,c}$). Observed modulations with periods comparable to those of the dominant tide (i.e. the M_2 tide with a period of 12 h, 25 min) are obtained with filtering techniques (i.e., straightforward running averages to obtain modulations with periods between approximately 9 and 15 h). Observed modulations are marked with the suffix o (e.g., $\Delta H_{s,o}$).

In Fig. 14 calculated and observed modulations of the wave height and absolute period are presented. This figure shows that observed modulations of the wave height and the absolute period ($\Delta H_{s,o}$ and $\Delta T_{a,o}$, dashed lines) in general are clearly larger than the calculated modulations ($\Delta H_{s,c}$ and $\Delta T_{a,c}$, solid lines), except for the modulations of the absolute period at Euro-0.

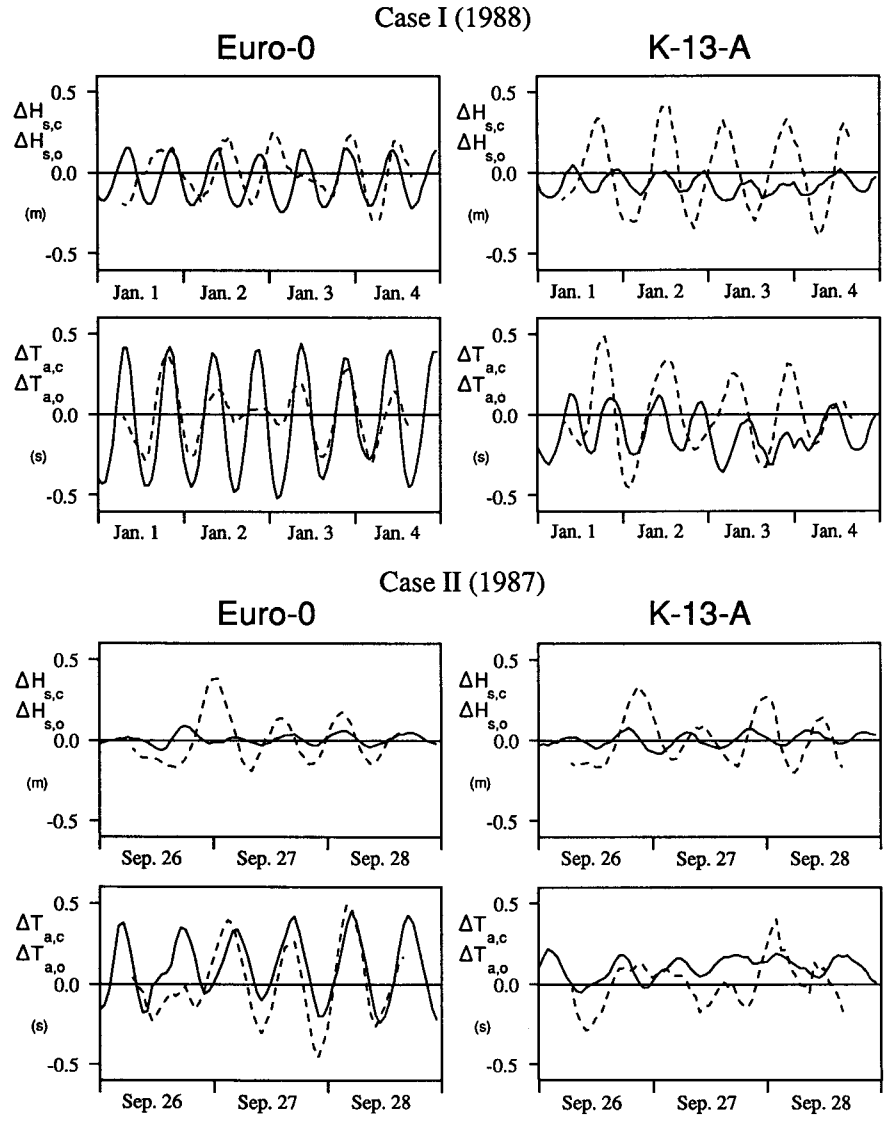

FIG. 14. Observed and calculated modulations of the significant wave height and the mean absolute period at Euro-0 and K-13-A for cases I and II. Solid line: calculated modulations; dashed line: observed modulations.

The residual modulations, defined as the difference between observed and calculated modulations ($\Delta H_{s,r} = \Delta H_{s,o} - \Delta H_{s,c}$ and $\Delta T_{a,r} = \Delta T_{a,o} - \Delta T_{a,c}$, respectively), might well be contributed to wind-induced modulations in the observations, in particular, since calculated tide-induced modulations are relatively small. Wind-induced modulations can obviously not be distinguished from tide-induced modulations by filtering techniques. Furthermore, wind-induced modulations cannot be calculated like tide-induced modulations, since sufficiently accurate (high resolution) wind fields are not available. Consequently, the hypothesis that the residual modulations are truly wind-induced, can only be checked by assessing their correlation with observed wind speed variations ΔU_{10} (obtained in a similar way as observed modulations of wave parameters). Since only local variations of the wind speed can be considered in such a comparison, good correlations between wind speed variations and their presumed effects on wave parameters are expected in conditions of active wave generation only. For the second half of the period of case II waves at Euro-0 and K-13-A consist for a major part of swell, so that a good correlation cannot be expected in this period, even if e.g., $\Delta H_{s,w}$ indeed is caused by wind speed variations.

Residual modulations of the wave height and absolute period are compared with wind speed modulations in Fig. 15. For an intercomparison wind and wave data are normalized with their rms value for the period considered (denoted as $\Delta\tilde{U}_{10}$, $\Delta\tilde{H}_{s,r}$, and $\Delta\tilde{T}_{a,r}$). This figure shows high correlations between residual modulations of the wave height $\Delta\tilde{H}_{s,r}$ and wind speed variations $\Delta\tilde{U}_{10}$, except (as expected) for the swell-dominated second half of case II. The correlation between residual modulations of the absolute period $\Delta\tilde{T}_{a,r}$ and wind speed variations $\Delta\tilde{U}_{10}$ is less pronounced but still clear (except for the second half of case II). It therefore appears that the residual modulations of mean wave parameters ($\Delta H_{s,r}$ and $\Delta T_{a,r}$) indeed are wind-induced and that the above differences between hindcast and observation are apparently not caused by model errors.

Figure 15 shows that the modulations of the wind speed have the character of noise rather than that of a systematic variation with a dominant frequency. Furthermore, the magnitude of the variations is 10% to 20% of the overall wind speed, so that these variations are not dominant. Consequently the wind speed modulations encountered here do not seem extraordinary and probably occur frequently in wind fields. Unfortunately wind speed variations on these time scales are usually not investigated by meteorologists.

The above wind speed variations are expected to occur in model wind fields commonly used in wave models (time steps of 3 h for example), but are poorly resolved in the time domain (four discrete values per tidal cycle only). Therefore, the above wind-induced modulations of mean wave parameters are expected to be poorly represented by present wave models.

4. Discussion

The results of the North Sea hindcasts presented here show that the unsteadiness of tidal currents has a significant influence on wave–tide interactions. As mentioned in the Introduction, this was expected, considering previous results for academic cases (Tolman 1990b) which, however, did not incorporate inhomogeneities related to the two-dimensional structure of the tide or to the bathymetry. In these academic cases, the relative importance of inhomogeneity is consequently smaller and the relative importance of unsteadiness is larger than in realistic conditions. The North Sea hindcasts of the present study show that unsteadiness remains important in realistic shelf sea conditions. Furthermore, the hindcasts show that the relative importance of unsteadiness and inhomogeneity varies in space and time so that effects of wave–tide interactions cannot be estimated from local depth and current parameters only, nor with a quasi-stationary or quasi-homogeneous approximation.

Whereas tide-induced modulations of wave periods are fairly well explained by the local and instantaneous relative importance of unsteadiness and inhomogeneity, modulations of wave heights are not yet fully explained. Figure 7 shows that in case I the larger current velocities at Euro-0 result in larger modulations of the wave height compared to K-13-A, as would be expected. However, in case II (and case III, figures not presented) tide-induced modulations of the wave height at K-13-A are larger than at Euro-0, in spite of the larger current velocities at the latter location. Furthermore, the wave height shows significant tide-induced modulations in case I, but only small modulations in cases II and III (compared to relative modulations of the periods). Apart from the wind direction and speed, there are two differences between the conditions of case I, on the one hand and cases II and III on the other hand, which might explain the above differences in wave height modulations. First, in case I the waves in the southern North Sea are locally generated, whereas for cases II and III waves are, for a significant part, generated in the central North Sea. Second, the waves in case I are essentially in deep water, whereas the waves in case III are depth-limited. Both local generation and relative depth (e.g., through variations in the energy dissipation due to bottom friction) might have a significant effect on tide-induced modulations of the wave height. With the present study, however, this cannot be investigated so that the above differences between the results for H_s of cases I, II and III cannot be explained satisfactorily.

The tidal currents result in modulations of mean wave parameters with an oscillating character (see e.g., Fig. 6), whereas currents and surface level variations of surges result in more monotonic variations (see e.g., Fig. 10). Wave–tide interactions seem to accumulate much less than wave–surge interactions, since case III

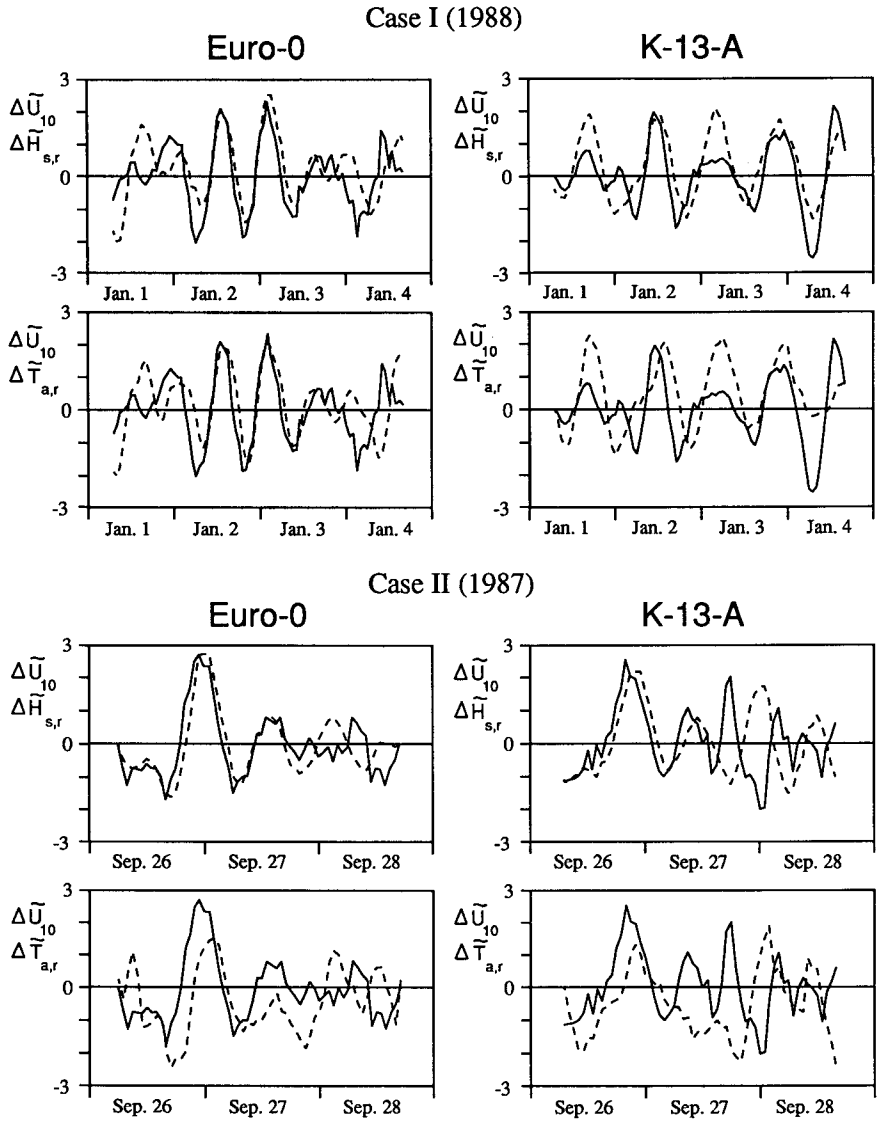

FIG. 15. Normalized filtered wind speeds (solid) and residual modulations of mean wave parameters (dashed) at Euro-0 and K-13-A for cases I and II.

shows that current-induced interactions appear to be surge dominated, although the local currents are clearly tide-dominated (as discussed in section 3c). In the storm surge case considered here, effects of currents and surface level variations largely cancel out and resulting relative modulations of mean wave parameters are much smaller than in the moderate cases. It might therefore be concluded that the relative importance of wave–tide and wave–surge interactions decreases with increasing storm severity. However, the cancelling out of the effects of currents and surface level variations cannot be expected to occur in any complex storm case. The potential magnitude of wave–surge interactions, therefore, is given by the potential magnitudes of the effects of water level variations and currents separately, which are roughly of the same order of magnitude as the effects of tides in the tide-dominated conditions considered here. Consequently, it cannot be concluded from the present results that the relative importance of interactions decreases with increasing storm severity.

This paper focuses on modulations of mean wave parameters. However, modulations of spectral densities or of energy in fixed frequency bands, in general, are much more pronounced than those of the mean wave parameters (modulations of 50% or more in all parts of the spectrum, e.g., Fig. 9). In particular, the effects of the tides and surges on the low-frequency variance (or energy) is striking, since wave–current interactions for monochromatic waves suggest a decreasing effect

of currents with decreasing frequency due to decreasing Doppler shifts kU_p and relative current velocities U/c_g. This large impact is explained from the steep gradients in the low-frequency flank of frequency spectra, where small shifts of the spectral peak frequency (or mean frequency) can cause large modulations of the total variance in fixed frequency bands. Like the frequency shifts, these modulations of spectral densities are strongly influenced by the unsteadiness of depth and current and cannot be estimated from local depth and current parameters only, or with conventional quasi-stationary approaches (as discussed above). The above (qualitative) results have been obtained for typical North Sea conditions, but they are believed to be fairly applicable to tides and surges in most shelf seas. The magnitude of interactions and the relative importance of wind speed variations in observed modulations, however, are expected to be relevant for the North Sea only.

Considering the relatively small magnitude of effects of wave–tide and wave–surge interactions on the significant wave heights, H_s, and the mean wave periods, T_a and T_r, (typically 5% to 10%), the implications for North Sea wave forecasting seem to be small. Such a conclusion is supported by the fact that observed modulations appear to be mainly wind-induced. However, the calculated modulations might be significant when assessing design wave heights for offshore platforms for example. Furthermore, the large modulations of spectral densities due to tides has implications for the dynamic analysis of structures, e.g., as is illustrated by a study of the wave-induced movements and accelerations of the Euro-0 platform (tide-induced modulations of the order of 50%, Peters and Boonstra 1988).

5. Conclusions

This study on effects of tides and storm surges on wind waves in the North Sea has given rise to the following conclusions. Tides and storm surges in shelf seas should be treated as an unsteady medium for wind wave propagation. Both the unsteadiness and the inhomogeneity of depth and current play a significant role in the interactions so that neither a quasi-stationary nor a quasi-homogeneous approximation to wave–current interactions can be used. In moderate wind and wave conditions interactions are predominantly caused by (tidal) currents, whereas in severe conditions both currents and (mean) surface level variations contribute to the interactions. Due to accumulation of effects, relatively small currents of surges might have larger impacts on mean wave parameters than larger (but oscillating) tidal currents. Although these conclusions are obtained from North Sea storm cases, they are expected to hold for tides and surges in other shelf seas.

For the North Sea the tide- and surge-induced modulations of mean wave parameters such as the significant wave height and the mean wave periods are relatively small (typically 5% to 10%). Tide-induced variations of spectral densities can be of the same order of magnitude as the average spectral density over a tidal period. In the three North Sea cases analyzed, observed modulations of mean wave parameters (in particular, wave height) appear to be wind-dominated rather than tide-dominated.

Acknowledgments. I want to express my gratitude to the Dutch Ministry of Public Works and Transportation (Rijkswaterstaat), in particular J. de Ronde, R. van Dijk, A. J. van der Kerk, and H. Ligtvoet, for supplying the bottom schematization of the North Sea, the tidal boundary conditions and observed wind and wave data. For supplying the wind fields, I want to express my gratitude to the Royal Netherlands Meteorological Institute (KNMI), in particular H. W. Riepma and E. Bouws. Permission to use an operational version of the numerical model DOLPHIN of Digital Hydraulics Holland B. V. is greatly appreciated. I would like to thank my colleagues at the Delft University of Technology, KNMI, Delft Hydraulics and Rijkswaterstaat, and members of the WAM group for their support, suggestions and comments, in particular L. H. Holthuijsen, J. A. Battjes and N. Booij. The help of L. Rumburg in preparing the figures was greatly appreciated. Part of this paper has been written while the author held a National Research Council—NASA Research Associateship.

REFERENCES

Barber, N. F., 1949: Behaviour of waves on tidal streams. *Proc. Roy. Soc. London,* **A 198,** 81–93.

Bretherthon, F. P., and C. J. R. Garrett, 1968: Wave trains in inhomogeneous moving media. *Proc. Roy. Soc. London,* **A 302,** 529–554.

Chen, Y. H., and H. Wang, 1983: Numerical model for nonstationary shallow water wave spectral transformations. *J. Geophys. Res.,* **88**(C14), 9851–9863.

Hasselmann, K., 1960: Grundgleichungen der Seegangsvoraussage. *Schiffstechnik,* 7 heft 39, 191–195.

Holthuijsen, L. H., and S. de Boer, 1988: Wave forecasting for moving and stationary targets. *Computer Modelling in Ocean Engineering,* B. Y. Schrefler and O. C. Zienkiewicz, Eds., Balkema, 231–234.

Jonsson, I. G., 1990: Wave-current interactions. *The Sea Volume 9: Ocean Engineering Science.,* B. Le Mehaute and D. M. Hanes, Eds., Wiley, and Sons.

Komen, G. J., S. Hasselmann and K. Hasselmann, 1984: On the existence of a fully developed wind—sea spectrum. *J. Phys. Oceanogr.,* **14,** 1271–1285.

Longuet-Higgins, M. S., and R. W. Stewart, 1960: Changes in the form of short gravity waves on long waves and tidal currents. *J. Fluid Mech.,* **8,** 565–583.

——, and ——, 1961: The changes in amplitude of short gravity waves on steady nonuniform currents. *J. Fluid Mech.,* **10,** 529–549.

——, and ——, 1962: Radiation stress and mass transport in gravity waves, with application to 'surf-beats'. *J. Fluid Mech.,* **13,** 481–504.

Madsen, O. S., Y.-K. Poon and H. C. Graber, 1988: Spectral wave attenuation by bottom friction: theory. *Proc. 21st Int. Conf. on Coastal Engineering,* ASCE, Malaga, 492–504.

Mei, C. C., 1983: *The Applied Dynamics of Ocean Surface Waves.* Wiley and Sons, 740 pp.

Peregrine, D. H., 1976: Interaction of water waves and currents. *Adv. Appl. Mech.,* **16,** 9–117.

——, and I. G. Jonsson, 1983: Interaction of waves and currents. Miscellaneous Rep. No. 83-6, CERC, U.S. Army Corps of Engineers.

Peters, H. C., and H. Boonstra, 1988: Fatigue loading on a single pile platform due to combined action of waves and currents. *Proc. 5th Int. Conf. on the Behaviour of Offshore Structures,* 1015–1034.

Phillips, O. M., 1960: On the dynamics of unsteady gravity waves of finite amplitude. Part I. *J. Fluid Mech.,* **9,** 193–217.

——, 1977: *The Dynamics of the Upper Ocean.* 2nd ed. Cambridge University Press, 336 pp.

Snyder, R. L., F. W. Dobson, J. A. Elliott and R. B. Long, 1981: Array measurements of atmospheric pressure fluctuations above surface gravity waves. *J. Fluid Mech.,* **102,** 1–59.

Tolman, H. L., 1988: Propagation of wind waves on tides. *Proc. 21st Int. Conf. on Coastal Engineering,* Malaga, 512–523.

——, 1989: The numerical model WAVEWATCH: a third generation model for the hindcasting of wind waves on tides in shelf seas. Communications on hydraulic and geotechnical engineering, Delft University of Technology, Rep. No. 82-2, 72 pp.

——, 1990a: Wind wave propagation in tidal seas. Communications on hydraulic and geotechnical engineering, Delft University of Technology, Rep. No. 90-1, 135 pp.

——, 1990b: The influence of unsteady depths and currents of tides on wind-wave propagation in shelf seas. *J. Phys. Oceanogr.,* **20,** 1166–1174.

——, 1991: A third-generation model for wind waves on slowly varying, unsteady and inhomogeneous depths and currents. *J. Phys. Oceanogr.,* **21,** 782–797.

Unna, P. J., 1941: White horses. *Nature,* **148,** 226–227.

——, 1942: Waves on tidal streams. *Nature,* **149,** 219–220.

——, 1947: Sea waves. *Nature,* **159,** 239–242.

van der Vlugt, A. J. M., 1984: Experiences with the WAVEC-buoy. *Proc. Symp. Description and Modelling of Directional Seas,* Denmark, Danish Hydraulic Institute and Danish Maritime Institute, Paper A3.

Voogt, L., 1985: Een getijmodel van de Noordzee gebaseerd op de JONSDAP-1976 meting. Rijkswaterstaat note WWKZ-84G.006. (in Dutch).

WAMDI Group, 1988: The WAM model—a third generation ocean wave prediction model. *J. Phys. Oceanogr.,* **18,** 1775–1810.

Wang, Z. B., 1989: Mathematical modelling of morphological processes in estuaries. Communications on hydraulic and geotechnical engineering, Delft University of Technology, Rep. No. 89-1, 204 pp.

Whitham, G. B., 1965: A general approach to linear and nonlinear dispersive waves using a Lagrangian. *J. Fluid Mech.,* **22,** 273–283.

——, 1974: *Linear and Nonlinear Waves,* Wiley, 636 pp.

Yamaguchi, M., Y. Hatada and J. Hayakawa, 1989: A Numerical model for refraction computation of irregular waves due to time varying currents and water depth. *Proc. of JSCE,* Vol. 405/II-11, 225–234. (in Japanese).

——, and Y. Hatada, 1990: A Numerical model for refraction computation of irregular waves due to time varying currents and water depth. *Proc. 22th Int. Conf. on Coastal Engineering,* ASCE, Delft.